International Journal of Heat and Fluid Flow 30 (2009) 88–98

Contents lists available at ScienceDirect

International Journal of Heat and Fluid Flow

journal homepage: www.elsevier.com/locate/ijhff

Air-lift pumps characteristics under two-phase flow conditions

Sadek Z. Kassab [a], Hamdy A. Kandil [a], Hassan A. Warda [a], Wael H. Ahmed [b,*]

[a] Mechanical Engineering Department, Faculty of Engineering, Alexandria University Alexandria, Egypt
[b] Nuclear Safety Solution Ltd., AMEC, 700 University Avenue, Toronto, Ontario, Canada M5G 1X6

ARTICLE INFO

Article history:
Received 31 March 2008
Received in revised form 22 September 2008
Accepted 23 September 2008
Available online 13 November 2008

Keywords:
Air-lift pumps
Two-phase flow
Vertical pipe

ABSTRACT

Air-lift pumps are finding increasing use where pump reliability and low maintenance are required, where corrosive, abrasive, or radioactive fluids in nuclear applications must be handled and when a compressed air is readily available as a source of a renewable energy for water pumping applications. The objective of the present study is to evaluate the performance of a pump under predetermined operating conditions and to optimize the related parameters. For this purpose, an air-lift pump was designed and tested. Experiments were performed for nine submergence ratios, and three risers of different lengths with different air injection pressures. Moreover, the pump was tested under different two-phase flow patterns. A theoretical model is proposed in this study taking into account the flow patterns at the best efficiency range where the pump is operated. The present results showed that the pump capacity and efficiency are functions of the air mass flow rate, submergence ratio, and riser pipe length. The best efficiency range of the air-lift pumps operation was found to be in the slug and slug-churn flow regimes. The proposed model has been compared with experimental data and the most cited models available. The proposed model is in good agreement with experimental results and found to predict the liquid volumetric flux for different flow patterns including bubbly, slug and churn flow patterns.

1. Introduction

The great focus towards the renewable energy for water pumping applications brought the attention to revisit the analysis of the air-lift pumps operated in two-phase flow. As the pneumatic transmission wind pumps operate on the principle of compressed air by using a small industrial air compressor to drive an air-lift pump or pneumatic displacement pumps. The main advantage of this method is that there is no mechanical transmission from the windmill to the pump, which avoids water hammer and other related dynamic problems. The pump can operate slowly even while the windmill is running rapidly with no dynamic problem. Other advantages are its simplicity and low maintenance. However, this technology is still under development and will require intensive field testing before it can be commercialized.

Air-lift pump is a device for raising liquids or mixtures of liquids and solids through a vertical pipe, partially submerged in the liquid, by means of compressed air introduced into the pipe near the lower end. The air then returns up in a discharge pipe carrying the liquid with it. The pump works by "aerating" the liquid in the discharge pipe. The added air lowers the specific gravity of the fluid mixture. Since it is lighter than the surrounding liquid, it is pushed upwards.

The principles of air-lift pumping were understood since about 1882, but practical use of air-lift did not appear until around the beginning of the twentieth century (Bergeles 1949). In comparison with other pumps, the particular merit of the air-lift pump is the mechanical simplicity. Moreover, they can be used in a corrosive environment, and are easy to use in irregularly shaped wells where other deep well pumps do not fit. Thus, theoretically, the maintenance of this kind of pumps has a lower cost and higher reliability. There is a wide use of the air-lift pumps in many applications such as in under water explorations or for rising of coarse particle suspensions (Stenning and Martin 1968), dredging of river estuaries and harbors, and sludge extraction in sewage treatment plant (Storch 1975).

The present study is concerned with the applications of air-lift pumps in pumping liquids. In this case, the flow in the pump riser is a two-phase flow. The flow of the two phases in the riser of an air-lift pump is a direct application of the upward flow in vertical round tubes. The common flow patterns for vertical upward flow are changing as the mass quantity is increased (Taitel et al. 1980).

Sharma and Sachdeva (1976) studied the factors that affect the performance of big diameter air-lift pumps operating in shallow depths. They related the pump performance to the type of flow pattern in the riser. In addition, DeCachard and Delhaye (1996) showed experimentally that the dominant flow pattern in the practical operating range of a small diameter air-lift pump is slug

* Corresponding author. Tel.: +1 6135846814; fax: +1 6135849497.
E-mail addresses: wael.ahmed@amec.ca, wael.ahmed@gmail.com (W.H. Ahmed).

0142-727X/$ - see front matter © 2008 Elsevier Inc. All rights reserved.
doi:10.1016/j.ijheatfluidflow.2008.09.002

Nomenclature

A	pipe cross-sectional area, m^2	W	weight, N
b	wetted perimeter of pipe	ρ	density, kg/m^3
D	pipe diameter, m	η	efficiency,%
f	friction factor	τ	wall shear stress, N/m^2
g	gravitational acceleration, m/s^2	ε	pipe roughness
H_s	static depth of water, m	R_e	Reynolds number
H_d	static lift		
K	friction parameter	*Subscripts*	
L	pipe length, m	1	entering injection zone
L_s	pipe suction length, m	2	leaving injection zone
P	pressure, N/m^2	a	atmospheric
Q	volume flow rate (discharge), m^3/s	gs	gas as a single phase
S_r	S_r = Hs/L, submergence ratio	g	gas
s	slip ratio	L	liquid
U	superficial velocity, m/s	ls	liquid as a single phase
V	velocity, m/s	S	solid

flow. A few studies are available on the effect of the liquid properties such as surface tension and viscosity and pipe geometry on the air-lift pump performance. For example, Khalil and Mansour (1990) carried out experimental work to study the effect of introducing a surfactant in the pumped liquid. They proved that the use of a surfactant in small concentration always increases the capacity and efficiency of the pump. Further, they found that the pump performance is a function of the volumetric air-flow rate, submergence ratio (Hs/L) as shown in Fig. 1, air-supply pressure and surfactant concentration. Iguchi and Terauchi (2001) studied the effect of the pipe-wall wettability on the transition among bubbly and slug flow regimes in air–water two-phase flow in a vertical pipe. They changed the advancing contact angle of an acrylic pipe by coating its inner wall by a hydrophilic substance or liquid paraffin. Some differences were observed between pipe walls of different wettability. Flow pattern maps were developed for different pipe-wall wettability. Also, Furukawa and Fukano (2001) investigated experimentally the effects of the liquid viscosity on the flow patterns of upward air–liquid two-phase flow in a vertical pipe. They used three different liquids including water and glycol solutions. They proposed flow pattern maps for each liquid viscosity. It was found that flow pattern transitions strongly depend on the liquid viscosity. Recently, Hitoshi et al. (2003) found experimentally that the gas-injection point has a big effect on discharged water. They concluded that, as gas-injection point increases above 45 pipe diameters, the discharged water decreases.

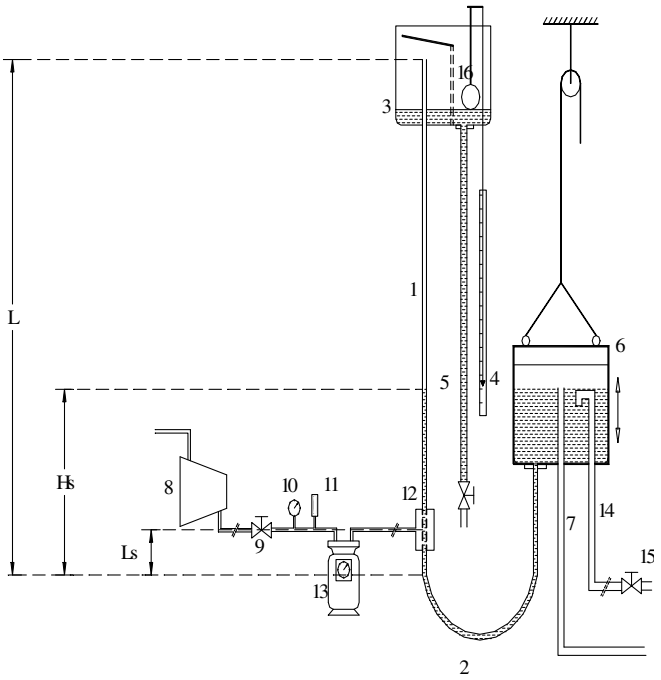

Fig. 1. A schematic diagram of the experimental setup. 1.Riser, 2. Down comer, 3. Overhead collecting tank, 4. Scale, 5. Drain, 6.Water feeding tank, 7. Over flow pipe, 8. Compressor, 9. Regulator, 10. Pressure gage, 11. Thermometer, 12. Air-jacket, 13. Below meter, 14. Feeding water line, 15. Control valve, 16. Float.

Although the geometry of the pump is very simple, the theoretical study of its performance is very complicated. The efforts to explain and study its performance started very early in the last century. Among the early classical theories of the air-lift pump, are those proposed by Harris, Lorenz, Gibson, and Swindin, as mentioned by Stapanoff (1929). Harris considered the force of buoyancy of the air bubbles as the motive force of the pump. He analyzed the motion of the bubble, and obtained the relation between the size of the bubble, slip (relative velocity of the air bubble with respect to the water), and the head produced. Lorenz, in developing his theory, wrote Bernoulli's equation for a differential head corresponding to a given flow in the discharge pipe, introducing variable pressure, density of mixture, and integrating between the head limits and thus he obtained the relation between the variables involved. Stapanoff (1929) used the thermodynamics theory in studying the effect of the submergence, the diameter of the riser pipe, air to water ratio, climate, and introducing compressed air above the surface of the water in the well, on the efficiency of the air-lift pump. He found that treating the air-lift pump thermodynamically has a definite advantage in explaining many points of its operation.

More than three decades later, a theoretical treatment of the air-lift pump, based on the theory of slug flow, was presented by Nicklin (1963). He studied the effects of different parameters including; diameter, length, pressure at the top of riser tube, submergence ratio, and water volumetric flow rate, on the air-lift-pump efficiency. He found that, by neglecting the entrance effects and assuming slug flow in the riser tube, the performance of the air-lift pump may be obtained based on two-phase slug flow regime. He used a definition of the efficiency of the pump as the work done in lifting the liquid, divided by the work done by the air as it expands isothermally. The theory presented by Nicklin was extended by Reinemann et al. (1986) taking into account the effect

of surface tension on the bubble velocity. Another analytical study of air-lift pump performance was presented by Stenning and Martin (1968). They used the continuity and momentum equations, assuming one-dimensional flow in the pump riser, and used the results of two-phase flow research to solve the governing equations. They found that one-dimensional-flow theory forms a good basis for the performance analysis of air-lift pumps. Also, Clark and Dabolt (1986) introduced a general design equation for air-lift pumps operating in slug flow regime by integrating the differential momentum equation over the whole pump length. The model was validated by the operation curves plotted from their experimental results. They indicated also that the analysis presented by Nicklin (1963) was accurate only in the design of short pumps, since there is no provision for variation in gas density over the tube length. In addition, they concluded that, the frictional pressure loss becomes significant for small riser diameter of about 10 mm.

The present study reviewed the previous models, dealt with the air-lift pump performance when operating in two-phase flow regime. A modified version of these models is developed. The results of the proposed modified model are then compared with the experimental measurements of Kassab et al. (2007) and other available models. In order to study the performance of the air-lift pump under different flow patterns the air-flow rate range was extended in the present study to cover different flow patterns including bubbly, slug, churn and annular flow conditions. In addition, pipes with different lengths were used to study the effect of the riser-pipe length, at the same submergence ratio, on the pump performance. Experiments were performed for nine submergence ratios, and three lengths of the pipe riser with different air injection pressures. Moreover, the different flow regimes and the transition of the flow patterns were observed and recorded and the results are discussed taking flow patterns into consideration.

2. Experimental setup

The experimental setup used in the present study is schematically shown in Fig. 1. It consists of a vertical transparent pipe (1), of 3.75 m length and 25.4 mm inner diameter, and a down-comer (2) of 30 mm inner diameter. The riser pipe is divided into three sections to allow studying the effect of changing the length of the riser pipe. The upper end of the riser is connected to an overhead-collecting tank (3) where the air escapes to atmosphere and water flow rate is measured according to the water level in the tank using a calibrated scale (4). The overhead tank is designed to absorb the water surface fluctuations and damp free vortices and thus provides accurate flow rate measurements. Water may be directed through a pipe (5) to the drain. The movable water supply tank (6) is kept at a constant water head by overflowing the water through a pipe (7). The tank may also be moved up or down to change the submergence ratio. All pipes and tanks are made of transparent material for visibility of the flow structure.

Air is supplied to the air injection system from a central air compressor station. The station consists of a 55 kW Ingersoll Rand screw compressor (8) delivering 8.2 m^3 of free air per minute at a maximum pressure of 8 bar, through a mass refrigeration dryer and filtration system, and an air reservoir of 3 m^3 capacity. Airflows from the air reservoir through a 25.4 mm diameter pipeline to an on/off valve, then to a pressure-reducing valve (regulator) (9), where the pressure is reduced to the desired working pressure (1×10^4–2.7×10^5 Pa) to cover the required experimental range. Air is then injected into the riser at a constant pressure that can be measured by the pressure gage (10). A mercury thermometer (11) is used for measuring the upstream air temperature. Then a constant air mass flow rate passes through an air jacket (12) around the vertical pipe using an air injector. The volume of air is measured using a calibrated below-meter (13). The air injector consists of 56 small holes of 3 mm diameter uniformly distributed around the pipe perimeter in seven rows and eight columns to insure uniform feed of the air into the pipe at the mixing section, which is 20 cm above the lower end of the pipe.

Various submergence ratios (from 0.2 to 0.75) were investigated in the present study. This range of submergence ratios was obtained in increments approximately 0.1, that covers most industrial applications where the air-lift pump is used. For each submergence ratio, the air-flow rate was varied and the corresponding flow rate of water was measured. In order to obtain specified and planed measurements, a specific operating procedure was followed for each run.

3. Results and discussion

3.1. Water flow rate

The results of lifting water in the riser tube of an air-lift pump, at various values of air mass flow rates corresponding to different values of air injection pressures are presented. Fig. 2 shows the water flow rate as a function of the air-flow rate at a submergence ratio of 0.4. Using flow visualization, Fig. 3, and the experimental results, it was noticed that for low values of air mass flow rate from 0 to 1 kg/h depends on the submergence ratio, no water is lifted due to the buoyant force exerted by the air bubbles is not enough to raise any water. The total quantity of air penetrates the water column without lifting any water. Fig. 3a shows that the flow regime is totally bubbly for very small values of air-flow rate. As the air mass flow rate is increased, a train of air slugs starts to develop in the pipe. It consists of some small slugs of lengths from 10 to 15 cm distributed along the pipe length. The biggest bubble is located at the upper part of the pipe while the smallest one is located at the lower part of the pipe. The train of air slugs moves slowly upwards leaving the pipe without any bubbles for a few seconds. The distribution is then repeated after a few seconds. This is because the air takes a few seconds to accumulate in the lower end of the pipe. It was observed that the air pressure at injection point fluctuates by 1 or 2 kPa around a mean value. This is due to the accumulation of air to form a slug that is strong enough to penetrate the water column and move upwards. When the air mass flow rate is increased slightly over 0.229 kg/h, the water flow starts, and the flow picture, Fig. 3b, is similar to the case of the penetrating column except that, the slugs become taller. The

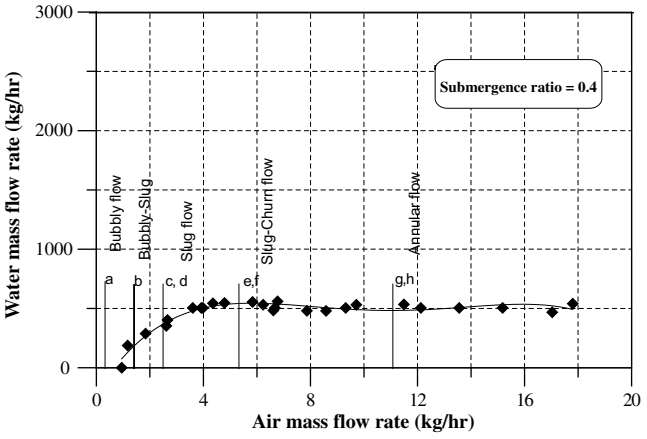

Fig. 2. Variation of air mass flow rate with water mass flow rate at submergence ratio = 0.4 (a–g represent the sequence of photos presented in Fig. 3).

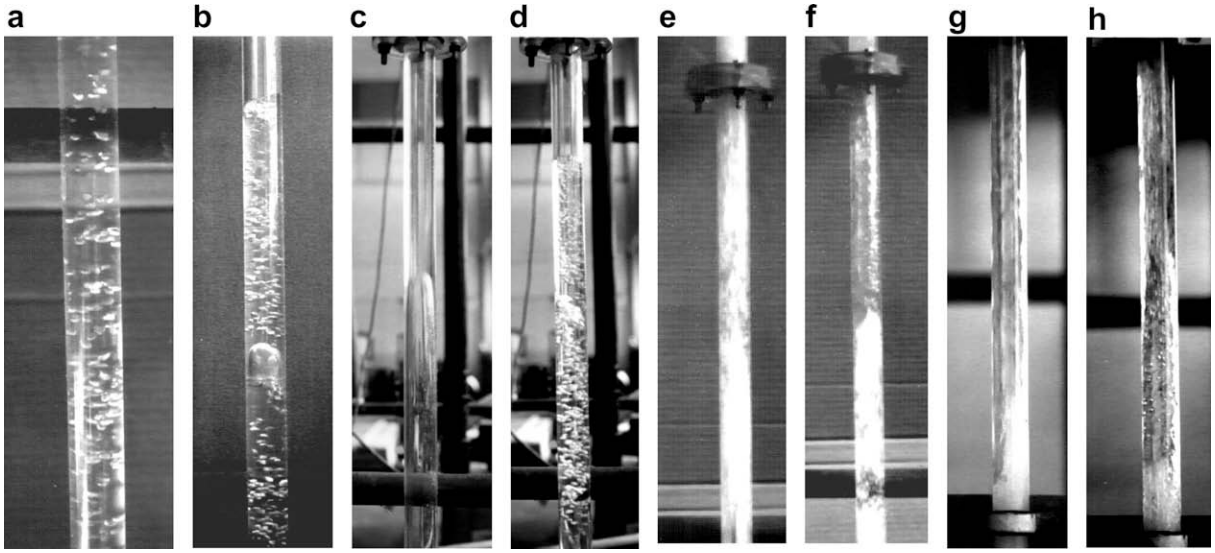

Fig. 3. Photos present the sequence of the flow patterns: (a) Bubbly, (b) bubbly to slug, (c and d) slug, (e and f) slug-churn, (g and h) annular.

structure of the slug flow in the pipe can be described by a sequence of a big air slug followed by a water slug that contains some small air bubbles and then smaller air and water slugs. The cycle is then repeated as shown in Figs. 3c–d. This observation agrees with the experimental work by Sekoguchi et al. (1981). This sequence of slug formation may be due to the time taken to charge enough quantity of air capable of lifting a certain amount of water. This explains the oscillation of the air injection pressure. The oscillation and the instability of the pump were studied by Hjalmars (1973). He found that, for a large air-lift pump, when the static lift was increased to about 30-40 pipe diameters, the instability of the air-lift pump starts. However, when the value of the static lift reached a critical value, instability sets in with a periodic and increasing variation of water discharge around its stationary value. The reason of these oscillations was also discussed by Sekoguchi et al. (1981). They referred this behavior to the compressibility of the gas in the gas–liquid two-phase mixture and reversal of water flow from the two-phase mixing section to the head tank. In the present study a very small variation was observed, and hence the instability effects were neglected.

The reason for the transition from bubbly to slug flow is that, as the gas flow is increased, the bubbles get closer together and collision occurs. Therefore, some of the collisions lead to coalescence of bubbles and eventually to the formation of slugs. For a submergence ratio of 0.75, the lifting of water becomes noticeable at a value of air-flow rate of approximately 1 kg/h. Any slight increase in the airflow rate beyond that value causes the water flow rate to increase rapidly. It is noted that in the region where the water mass flow rate is increasing (from 403 to 642 kg/h), the flow regime is mostly slug-churn flow. In addition, the maximum flow rate of water (642 kg/h) occurs when the flow pattern is slug-churn flow.

As can be seen in Fig. 2, the water mass flow rate increases as the air mass flow rate increased, until it reaches a maximum value. It was noticed that, in the region in which the water flow rate increases, the flow pattern changed from slug to slug-churn flow as shown in Fig. 3e–f. This can be explained as follows: as the gas slug rises through the liquid, the direction of gas velocity inside the slug is upwards, while the water velocity direction in the thin film around the air slug is usually downwards, so the flow is counter current. At some critical value of air mass flow rate the gas velocity will suddenly disrupt the liquid film (the film will flood) and therefore the slug flow will break down to give churn flow with pulsating, highly unstable pattern, as suggested by Nicklin (1963). It is noted that the region of the slug-churn flow is the main region where the pump should be operating. The quantity of lifted water remains almost constant for a small range of air-flow rates (from 5.3 kg/h to 6.2 kg/h). Physically, the maximum water flow rate is reached when the frictional pressure drop caused by further addition of air exceeds the buoyancy effect of the additional air, as was explained by Reinemann et al. (1986). Further increase in the airflow causes a slight decrease in the water flow rate to a value of (51 kg/h), and the flow regime changes from slug-churn to annular flow type as shown in Fig. 3g. This transition is because the gas velocity becomes high enough to support the liquid as a film on the tube wall, and also because the pressure drop exceeds the buoyancy effect.

Fig. 3h shows the annular flow pattern and also how water is lifted through the pipe riser. A small amount of water is transported as a liquid film on the tube walls, while another part forms small droplets of water injected in the pipe core upward. Measurements were performed at different values of submergence ratios, and the results are shown in Fig. 4. It is clear that the performance curves of the air-lift pump are shifted upward while the submergence ratio is increased. All the performance curves at different

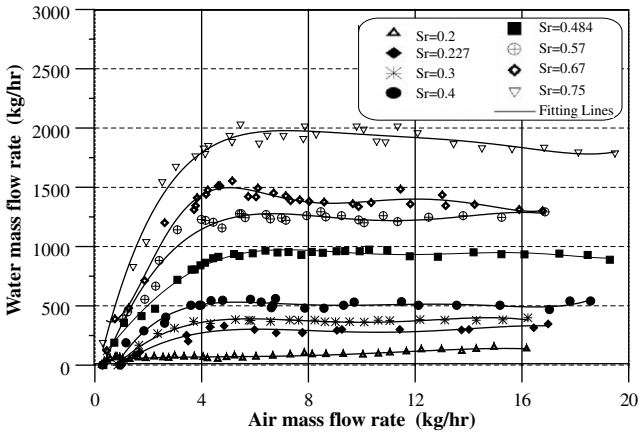

Fig. 4. Variation of water mass flow rate with air mass flow rate at different values of submergence ratio.

values of submergence ratio have similar trend. Also, during the experiments, it was noticed that the flow pattern changes by the same sequence as indicated earlier (for the 0.4 submergence-ratio case). In addition, Fig. 4 shows that, for a fixed value of air mass flow rate, the water flow rate increases with the increase of the submergence ratio.

3.2. The pump efficiency

The definition of the air-lift pumps efficiency is given by Nicklin (1963) as

$$\eta = \frac{\rho g Q_L (L - H_s)}{P_a Q_a Ln \frac{P_{in}}{P_a}}$$

where Q_L is the water discharge, Q_a is the volumetric flow rate of air, P_{in} the injection pressure of air, ρ is the liquid density and P_a is the atmospheric pressure.

Pump efficiency versus air mass flow rate, for a submergence ratio of 0.4, is shown in Fig. 5a. As the air mass flow rate is increased, the efficiency increases rapidly from 0 to reach a maximum value of 32.4% at an air mass flow equals 1.5 kg/h, and then, it tends to decrease as the air mass flow rate is increased.

The efficiency curves at different values of submergence ratio are presented in Fig. 5b. They have similar trend as the one presented in Fig. 5a for submergence ratio of 0.4. In addition the best efficiency range is in the first region of the performance curve, which is a slug flow region. The maximum efficiency increased to 44% when the submergence ratio is increased to 0.75 as presented in Fig. 5b. Comparing the water mass flow rate results presented in Fig. 4 with the efficiency results presented in Fig. 5, it is important to notice that, the maximum efficiency does not occur at the maximum water mass flow rate for all values of submergence ratio.

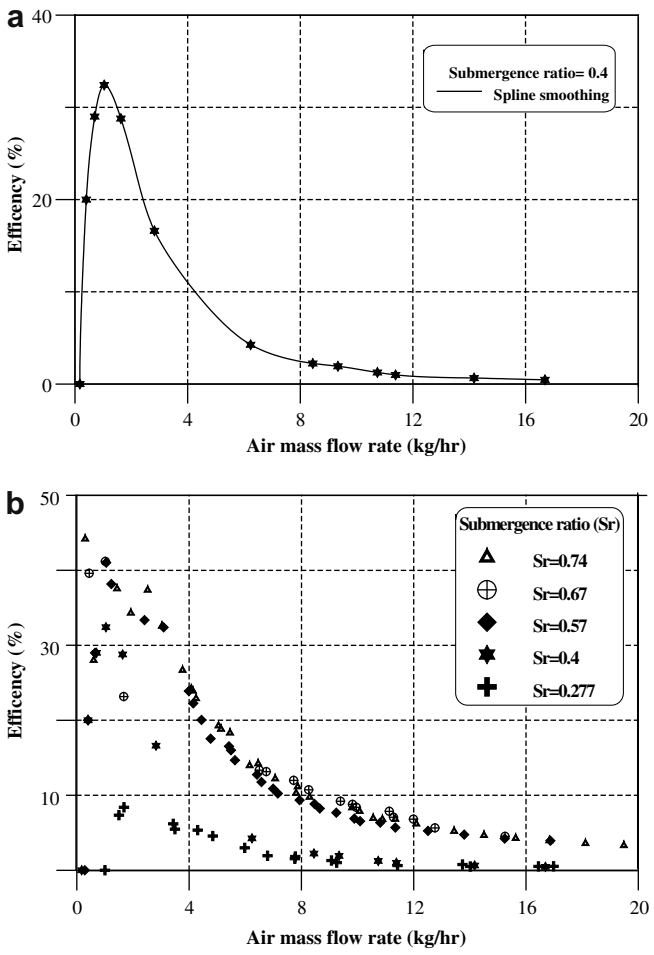

Fig. 5. Variation of pump efficiency with air mass flow rate at: (a) submergence ratio = 0.4 (b) different values of submergence ratio.

3.3. Effect of riser length

The effect of riser length was also studied in the present study. This was done by fixing the submergence ratio and varying the static lift by changing the riser length. Experiments were performed for submergence ratio values of 0.4, 0.484, 0.5, 0.57, 0.67, and 0.74, and different total pipe lengths of; 175 cm, 275 cm, and 375 cm. The performance curves of the pump are presented for each case in Fig. 6. While the effect of the variation of the static lift on pump efficiency for submergence ratio equal to 0.57, is shown in Fig. 7. It is clear from these figures that, for any riser length, there is a slight effect of the total pipe length on the performance pattern, in the slug flow region. However, the maximum water mass flow rate decreases when the static lift is decreased, and the performance curve shifts down by a small amount for the remaining regions. Moreover, for submergence ratios lower than 0.3, it was noticed that, there was no water lifted if the static lift is increased to 82.5 cm (32 pipe diameters). This is because air was not able to carry the water column to a distance equal to the static lift, and air penetrates the water column without lifting an accountable mass of water. The results presented in Figs. 6 and 7 show that not only the submergence ratio affects the air-lift pump performance but also the magnitude of the riser length.

3.4. Flow pattern map

Fig. 8a shows the distribution of the test data on the flow pattern map proposed by Taitel et al. (1980). It can be seen that the regions occupied by the experimental data points agree with the observations. Some experimental measurements from the high efficiency range ($\eta > 20\%$) at different submergence ratios are mapped on the flow-pattern map as shown in Fig. 8b. The best efficiency range where the efficiency exceeds 20% lies totally in the slug or slug-churn flow regions. This may explain why most analytical studies were based on the slug or slug-churn flow patterns.

4. Modeling the air-lift pump performance

The problem considered is the prediction of the liquid mass flow rate as a function of the air mass flow rate. The geometric parameters (L, H_s, L_s, and D), the pressure conditions (P_a, P_{in}), and the fluid properties are given as input data to the theoretical model equations. Where L is the riser-pipe length, H_s is the static head of water, L_s is the length of the suction part of the pipe, D is the pipe diameter, P_a is the atmospheric pressure, and P_{in} is the injection pressure to the riser pipe. As the basic performance data of the air-lift pump is computed, secondary results such as the efficiency may easily be determined.

4.1. Clark and Dabolt model

The general design equation for air-lift pumps operating in the slug flow regime that was developed by Clark and Dabolt (1986) is taken as a preliminary investigation model of the pump performance. A computer program was developed for the equations derived by Clark and Dabolt (1986), using the momentum balance. Derivation is based on the assumption that the two-phase flow remains within the slug flow mode and the flow is one-dimensional.

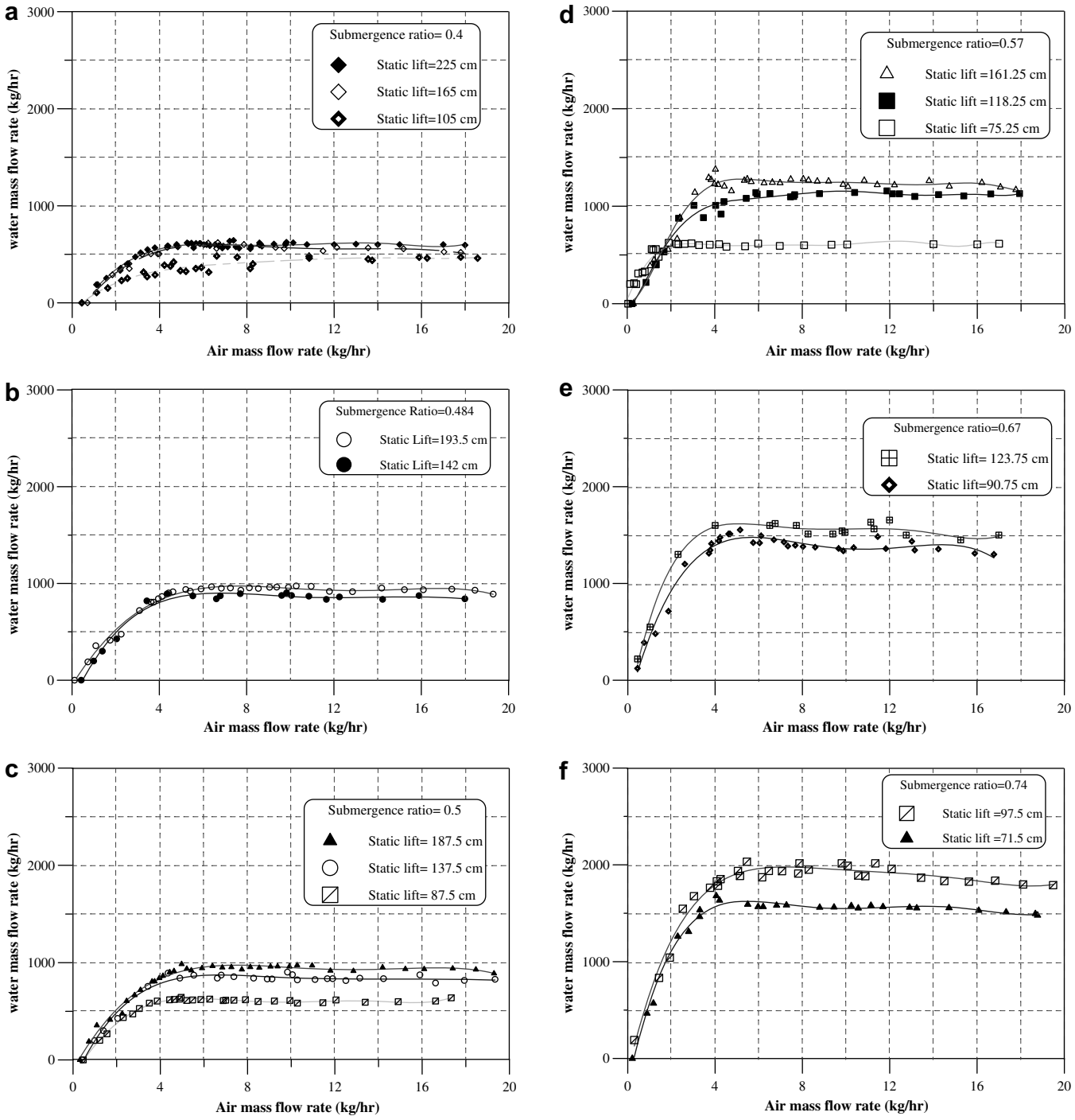

Fig. 6. Effect of static lift on the air-lift pump performance at various values of submergence ratio.

The theoretical predictions using Clark and Dabolt model together with the corresponding experimental results of Kassab et al. (2001) are presented in Fig. 9 for a submergence ratio of 0.4. The agreement between these two results is quite reasonable up to an air mass flow rate of 3.4 kg/h. The theoretical model does not predict the experimental data for air mass flow rates higher than 3.4 kg/h. The results obtained for different submergence ratios (not shown), were also compared with those predicted by the model proposed by Clark and Dabolt (1986). The comparison showed that the model is suitable only for the first region of pump performance, where the flow regime is slug. From the previous comparison and in order to extend the operating range of the air-lift pump, it is essential to develop a model which is more general than that proposed by Clark and Dabolt (1986).

4.2. A modified model for the performance of the air-lift pumps

As discussed earlier in the literature review, the direct approach to study the air-lift pump performance employs the momentum equation and the continuity equation, assuming one-dimensional flow. This assumption is valid for the practical operating range of the air-lift pumps as concluded by Clark and Dabolt (1986).

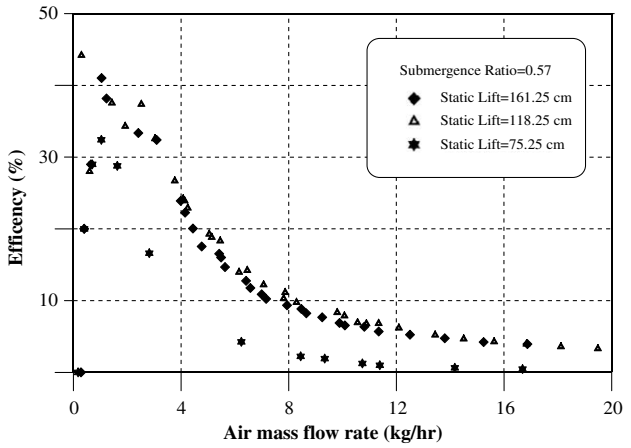

Fig. 7. Variation of the pump efficiency with the static lift at submergence ratio = 0.7.

Consider a vertical pipe partly full of liquid, and let the base of the pipe have a reference height of zero as shown in Fig. 10. Since the tube is filled to a static head of H_s, then the static pressure, P_o, at the base of the pipe is given by Bernoulli's equation as follows:

$$P_o = P_a + \rho_L g H_s - \frac{1}{2}\rho_L V_1^2 \quad (1)$$

where ρ_L is the liquid density, P_a is the atmospheric pressure and V_1 is the water velocity at the inlet section.

Neglecting the density changes of the air, the continuity equation can be written as follows:

$$AV_2 = Q_g + Q_L = Q_g + AV_1 \quad (2)$$

where V_2 is the mixture velocity of air and water leaving the injector.

Dividing all terms of Eq. (2) by $Q_L = AV_1$, gives

$$V_2 = V_1\left(1 + \frac{Q_g}{Q_L}\right) \quad (3)$$

Neglecting the air mass flow rate compared to the liquid mass flow rate, the continuity equation can be written as follows:

$$\rho_2 AV_2 = \rho_L AV_1 \quad (4)$$

So,

$$\rho_2 = \rho_L \frac{V_1}{V_2} \quad (5)$$

Substituting Eq. (3) in Eq. (5), we obtain

$$\rho_2 = \frac{\rho_L}{\left(1 + \frac{Q_g}{Q_L}\right)} \quad (6)$$

The momentum equation applied to the injector as a control volume, neglecting the wall friction, is given by

$$P_2 = P_o - \rho_L V_1 (V_2 - V_1) \quad (7)$$

From Eq. (3) in (7), then

$$P_2 = P_o - \frac{\rho_L V_1 Q_g}{A} \quad (8)$$

Hence, combining (1) and (8), gives

$$P_2 = P_a + \rho_L g H_s - \frac{1}{2}\rho_L V_1^2 - \frac{\rho_L V_1 Q_g}{A} \quad (9)$$

Neglecting momentum changes caused by the flow adjustment after the mixer, the momentum equation for the upper portion of the pump can be written as suggested by Stenning and Martin (1968) in the form:

$$P_2 - P_a = \tau \frac{Lb}{A} + \frac{W}{A} \quad (10)$$

where τ is the average wall shear stress, b is the wetted perimeter of the pipe, and W is the total weight of the gas and liquid in the pipe.

An expression for the average shear stress, τ, was suggested by Griffith and Wallis (1961) as follows:

$$\tau = f\rho_L\left(\frac{Q_L}{A}\right)^2\left(1 + \frac{Q_g}{Q_L}\right) \quad (11)$$

where f is the friction factor assuming that the water alone flows through the pipe.The weight of the fluid in the pipe equals the total weight of liquid plus gas, which can be obtained as follows:

$$W = L(\rho_L A_L + \rho_g A_g) \quad (12)$$

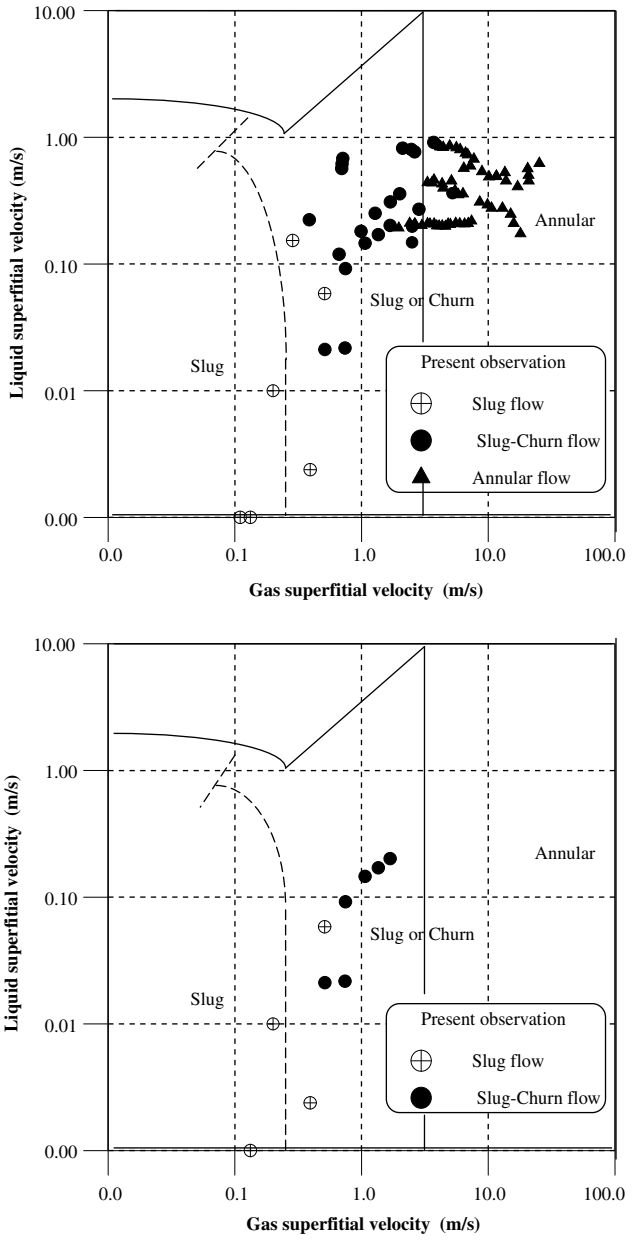

Fig. 8. Comparison between the results of the present study and Taitel et al. (1980) flow-pattern map: (a) distribution of the experimental data (b) distribution of the best efficiency points.

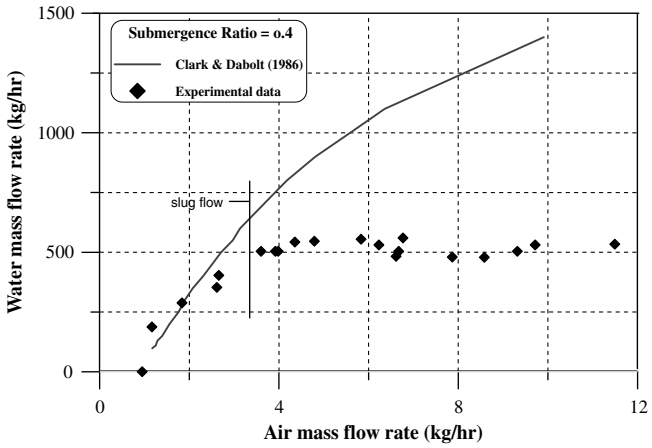

Fig. 9. Comparison between the results of Clark and Dabolt (1986) and the experimental results of Kassab et al. (2001).

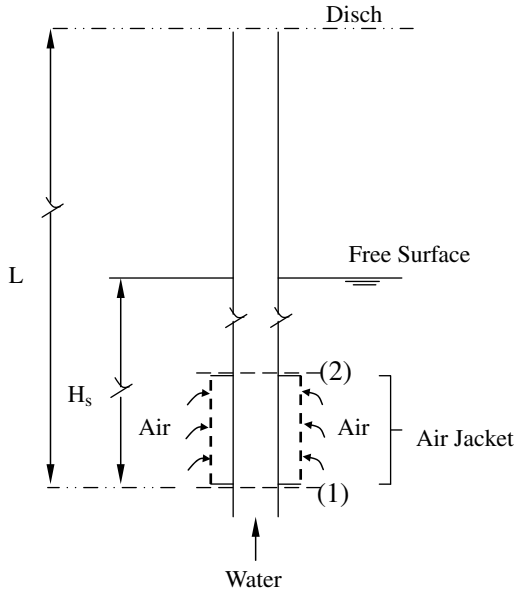

Fig. 10. Model for analysis of airlift pump.

where A_L is the area for the liquid phase, and A_g is the area for the gas phase.

$$A = A_L + A_g \tag{13}$$
$$Q_g = A_g V_g \tag{14}$$
$$Q_L = A_l V_L = A V_1 \tag{15}$$

Substituting (13)–(15) in (12) and neglecting the density of gas with respect to the liquid density, we obtain:

$$W = L\frac{\rho_L A}{\left(1+\frac{Q_g}{sQ_L}\right)} \tag{16}$$

where s is the slip ratio which equals:

$$s = \frac{V_g}{V_L} \tag{17}$$

where V_g and V_L are the actual velocities of gas and liquid, respectively.

Substituting from Eqs. (11) and (16) in Eq. (10), we get:

$$P_2 = P_a + \frac{4fL}{D}\rho_L V_1^2\left(1+\frac{Q_g}{Q_L}\right) + \rho_L \frac{L}{\left(1+\frac{Q_g}{sQ_L}\right)} \tag{18}$$

This equation was obtained by Stenning and Martin (1968) and it can be written as follows

$$\frac{H_s}{L} - \frac{1}{\left(1+\frac{Q_g}{sQ_L}\right)} = \frac{V_1^2}{2gL}\left[(K+1)+(K+2)\frac{Q_g}{Q_L}\right] \tag{19}$$

where K is the friction factor which is given by

$$K = \frac{4fL}{D} \tag{20}$$

Stenning and Martin (1968) used the above equations in their analytical model but they fixed the values of the slip ratio (s), and the friction factor (K). Physically, the slip ratio changes as the water mass flow rate and air mass flow rate changes. Also, the friction factor changes with changing the flow conditions.

In the present work, the slip ratio is considered as a function of the water and air mass flow rates as expressed by Griffith and Wallis (1961) for slug flow in the form:

$$s = 1.2 + 0.2\frac{Q_g}{Q_L} + \frac{0.35\sqrt{gD}}{V_1} \tag{21}$$

Also, the friction factor is obtained using Colebrook equation as listed by Haaland (1983), where the friction factor, f, may be obtained by solving the following equation:

$$\frac{1}{\sqrt{f}} = -2.0log\left(\frac{\varepsilon/D}{3.7}+\frac{2.51}{Re\sqrt{f}}\right) \tag{22}$$

where ε is the pipe roughness and Re is the Reynolds number.

Finally, the pump efficiency is calculated in the present study using the definition given by Nicklin (1963) as follows:

$$\eta = \frac{\rho g Q_L (L - H_s)}{P_a Q_a \ln\frac{P_{in}}{P_a}} \tag{23}$$

where Q_L is the water discharge, Q_a is the volumetric flow rate of air, P_{in} is the injection pressure of air, and P_a is the atmospheric pressure.

The modified model is obtained by inserting Eqs. (21) and (22) in Eq. (19). Using this modified model, a computer program was developed in order to investigate the air-lift pump performance over an extended range of the pump operation. A calculation procedure to obtain the results using the proposed model as follows:

(1) The geometrical parameters of L, D, pipe roughness ε, and the water density ρ and viscosity μ, are known. Then for a known air inlet pressure the inlet air mass flow rate is assigned.
(2) Select a static head Hs for a certain submergence ratio.
(3) Assume a value of water mass flow rate.
(4) Compute the coefficient of the friction f from Colebrook Eq. (22), also calculate the slip ratio "s" from Eq. (21).
(5) Calculate the value of friction factor "K" from Eq. (20).
(6) Calculate the value of the left hand side and the right hand side of Eq. (19).
(7) Repeat steps 3–6 until the total difference between the left hand side and the right hand side of (19) becomes less than 0.001.

5. Comparison with the experimental data

In order to evaluate the validity of the results obtained using the proposed model a comparison with the experimental results of

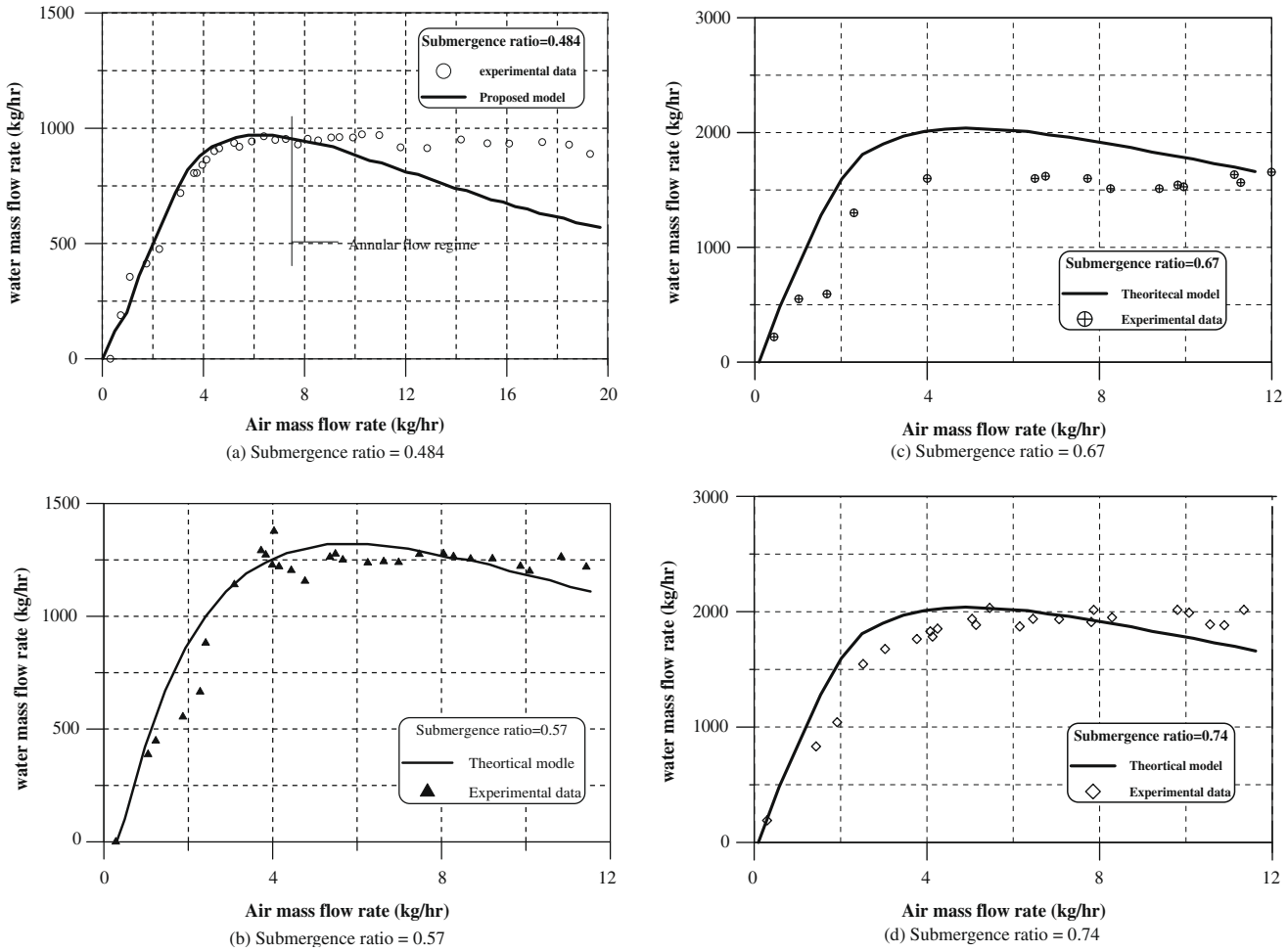

Fig. 11. Comparisons between the proposed model and the experimental results of Kassab et al. (2001).

Kassab et al. (2001) was performed. This comparison is shown in Fig. 11a for a submergence ratio of 0.484. It is clear from this figure that the agreement between the results of the proposed model and the experimental data is good over a range of air mass flow rates up to 8.3 kg/h while there is a large deviation for the remainder of the pump performance curve. This is due to the transition to the annular flow regime that is not taken into account in the present model.

More comparisons between the results of the proposed model and the experimental results obtained by Kassab et al. (2001), for some other submergence ratios, are shown in Figs. 11b–d. In general, good agreement is obtained for all presented submergence ratios. In addition, comparing the results presented in Fig. 9 with those in Fig. 11, one notices that the agreement of the present modified model with the experimental data is better than that of Clark and Dabolt (1986).

The average deviation based on root mean square values between the results of the present model and the experimental results is about 15%, which is acceptable if the model is used to investigate the performance in practical applications. It appears that the one-dimensional theory forms a good basis for the performance analysis of air-lift pumps.

The influence of the riser pipe length on the airlift performance was also studied using the modified model. Fig. 12 shows the effect of the riser pipe length on the air-lift pump performance in both theoretical and experimental results. It is noted that, the model

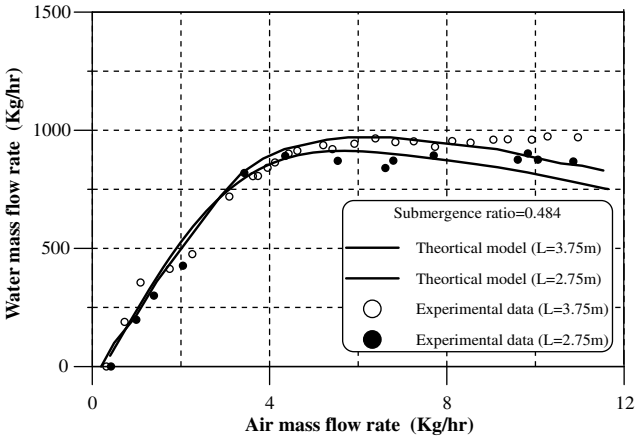

Fig. 12. Effect of the riser pipe length on the airlift-pump performance.

proposed in the present study senses well the change of riser pipe length.

The efficiency of the air-lift pump is computed using the present model based on the definition presented by Nicklin (1963). The obtained results are presented in Fig. 13 and are compared with the experimental results of Kassab et al. (2001). Good agreement between the theoretical and experimental results is achieved.

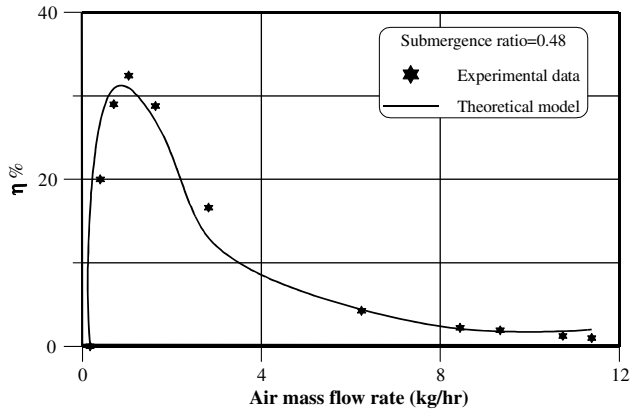

Fig. 13. Comparison between the calculated efficiency and that obtained experimentally by Kassab et al. (2001).

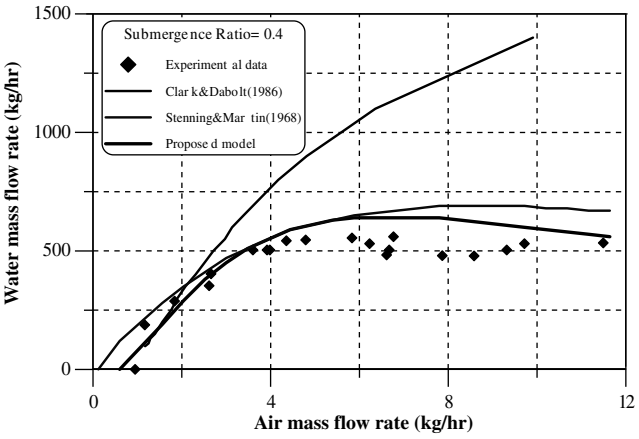

Fig. 14. Comparison between the results of various models and the experimental results of Kassab et al. (2001).

5.1. Comparison with other models

Fig. 14 shows a comparison between the results of the proposed model and the corresponding results obtained using Clark and Dabolt (1986) as well as Stenning and Martin (1968) models. It is clear from the comparison that the proposed model gives better agreement with the experimental data than especially in the best efficiency range while it is over predicting the experimental data in the annular flow pattern region. The range of model applicability is taken as acceptable error between the experimental data and the model predictions. In the present experimental range (air mass flow rate between 0 and 12 kg/h), the model found to be predict the water mass flow rate within 15% based on the root mean square. This difference found to increase as the flow pattern changes to annular flow. Also, the proposed model tends to predict the point where the pump starts to operate much better than the other two models.

6. Uncertainty analysis

The uncertainty analysis was performed according to the multivariate Taylor Series method and summarized in Table 1

$$U_R = \left[\left(\frac{\partial R}{\partial X_1}U_{X_1}\right)^2 + \left(\frac{\partial R}{\partial X_2}U_{X_2}\right)^2 + \cdots + \left(\frac{\partial R}{\partial X_J}U_{X_J}\right)^2\right]^{1/2} \quad (24)$$

Table 1
Uncertainty of the measured variables

Quantity	Percentage uncertainty (%)
Air mass flow rate	2.5
Water mass flow rate	4
Pressure	3
Temperature	2.5

where U_X is the uncertainty in the measured variable X. Also, the uncertainty for a measuring instrument is calculated from:

$$U_X = \sqrt{e_o^2 + e_c^2} \quad (25)$$

where e_o is the interpolation error, e_c is the instrument error

$$e_o = \pm\frac{1}{2} \times Re \text{ solution} \quad (26)$$

For example the procedures of calculating the uncertainty of the measured variable are as follows:

7. Concluding remarks

The following concluding remarks can be deduced from the present study:

- As the submerged ratio increases, the maximum efficiency of the pump increases at the same air-flow rate.
- The air-lift pump lifted maximum amount of liquid if operated in the slug or slug-churn regimes.
- The maximum efficiency does not occur at the maximum water mass flow rate.
- The best efficiency points always located in the slug or slug-churn flow patterns.
- For the same submergence ratio, varying the length of the riser pipe affects the air-lift pump performance.
- The one-dimensional model proposed in the present study can predict the air-lift pump performance and it can be used in the design of air-lift pumps for different flow patterns including bubbly, slug and churn flow patterns.
- The proposed model gives a good agreement with the experimental results within the practical range of operation of the air-lift pumps.

References

Bergeles, A.E., 1949. Flow of gas–liquid mixture. Chem. Eng., 104–106.
Clark, N.N., Dabolt, R.J., 1986. A general design equation for air-lift pumps operating in slug flow. AICHE J. 32, 56–64.
DeCachard, F., Delhaye, J.M., 1996. A slug-churn flow model for small diameter air lift pumps. Int. J. Multiphase Flow 22, 627–649.
Furukawa, T., Fukano, T., 2001. Effects of liquid viscosity on flow patterns in vertical upward gas–liquid two-phase flow. Int. J. Multiphase Flow 27, 1109–1126.
Griffith, P., Wallis, G.B., 1961. Two-phase slug flow. J. Heat Transfer, Trans. ASME 83, 307–320.
Haaland, S.E., 1983. Simple and explicit formulas for the friction factor in turbulent flow. J. Fluids Eng. 103, 89–90.
Hitoshi, F., Satoshi, O., Hirohiko, T., 2003. Operation performance of a small air-lift pump for conveying solid particles. J. Energy Resour. Technol. 125, 17–25.
Hjalmars, S., 1973. The origin of instability in air lift pumps. J. Appl. Mech. Trans. ASME 95, 399–404.
Iguchi, M., Terauchi, Y., 2001. Boundaries among bubbly and slug flow regimes in air–water two-phase flows in vertical pipe of poor wettability. Int. J. Multiphase Flow 27, 729–735.
Kassab, S.Z., Kandil, H.A., Warda, H.A., Ahmed, W.H., 2001. Performance of an air lift pump operating in two-phase flow. In: Proceedings of ICFDP7: The Seventh International Congress on Fluid Dynamics & Propulsion, December 18–20, 2001, Cairo, Egypt, Paper No. ICFDP7-2001004.

Kassab, S.Z., Kandil, H.A., Warda, H.A., Ahmed, W.H., 2007. Experimental and analytical investigations of airlift pumps operating in three-phase flow. Chem. Eng. J. 131, 273–281.

Khalil, M.F., Mansour, H., 1990. Improvement of the performance of an air lift pump by means of surfactants, Presented at the Sixth International Symposium of Heat and Mass Transfer, Miami, FL, USA.

Nicklin, D.J., 1963. The air lift pump theory and optimization. Trans. Inst. Chem. Eng. 41, 29–39.

Reinemann, D.J., Patrlange, J.Y., Timmons, M.B., 1986. Theory of small diameter air lift pump. Int. J. Multiphase Flow 16, 337–355.

Sekoguchi, K., Matsumura, K., Fukano, T., 1981. Characteristics of flow fluctuation in natural circulation air lift pum. JSME 14, 1960–1966.

Sharma, N.D., Sachdeva, M.M., 1976. An air lift pump performance study. AICHE J. 32, 61–64.

Stapanoff, A.J., 1929. Thermodynamic theory of air-lift pump. ASME 51, 49–55.

Stenning, A.H., Martin, C.B., 1968. An analytical and experimental study of air lift pump performance. J. Eng. Power, Trans. ASME 90, 106–110.

Storch. B., 1975. Extraction of sludges by pneumatic pumping. In: Second Symposium on Jet Pumps and Ejectors and Gas Lift Techniques, Churchill College, Cambridge, England, G4, pp. 51–60.

Taitel, Y., Bornea, D., Dukler, A.E., 1980. Modeling flow pattern transition for steady upward gas–liquid flow in vertical tubes. AICHE J 26, 345–354.